Phosphorylated Insulin-Like Growth Factor-I/Insulin Receptor Is Present in All Breast Cancer Subtypes and Is Related to Poor Survival

Jennifer H. Law,[1] Golareh Habibi,[1] Kaiji Hu,[1] Hamid Masoudi,[1] Michelle Y.C. Wang,[1] Anna L. Stratford,[1] Eugene Park,[1] Julia M.W. Gee,[2] Pauline Finlay,[2] Helen E. Jones,[2] Robert I. Nicholson,[2] Joan Carboni,[3] Marco Gottardis,[3] Michael Pollak,[4] and Sandra E. Dunn[1]

[1]Laboratory for Oncogenomic Research, Departments of Pediatrics, Experimental Medicine, and Medical Genetics, Child and Family Research Institute, University of British Columbia, Vancouver, British Columbia, Canada; [2]Tenovus Centre for Cancer Research, Welsh School of Pharmacy, Cardiff University, Cardiff, Wales, United Kingdom; [3]Bristol-Myers Squibb Oncology Drug Discovery, Princeton, New Jersey; and [4]Department of Oncology, Lady Davis Research Institute of the Jewish General Hospital and McGill University, Montreal, Quebec, Canada

Abstract

Drugs that target the insulin-like growth factor-I receptor (IGF-IR) and/or insulin receptor (IR) are currently under investigation for a variety of malignancies including breast cancer. Although we have previously reported that IGF-IR expression in primary breast tumors is common, the activation status of this receptor has not been examined in relation to survival. Phosphorylated IGF-IR/IR (P-IGF-IR/IR) and its downstream signaling partner phospho-S6 (P-S6) were evaluated immunohistochemically in tumor tissue microarrays representing 438 cases of invasive breast cancer. P-IGF-IR/IR (n = 114; P = 0.046) and total levels of IR (n = 122; P = 0.009) were indicative of poor survival, whereas total IGF-IR (n = 112; P = 0.304) was not. P-IGF-IR/IR and P-S6 were coordinately expressed in primary breast tumors (likelihood ratio, 11.57; $P = 6.70 \times 10^{-4}$). Importantly, P-IGF-IR/IR was detected in all breast cancer subtypes (luminal, 48.1%; triple negative, 41.9%; and HER2, 64.3%). *In vitro*, the IGF-IR/IR inhibitor BMS-536924 decreased phospho-RSK and P-S6, and significantly suppressed the growth of breast cancer cell lines MCF-7, SUM149, and AU565 representing the luminal, triple negative, and HER2 subtypes, respectively, in monolayer and soft agar. BMS-536924 also inhibited growth in tamoxifen resistant MCF-7 Tam-R cells while having little effect on immortalized normal breast epithelial cells. Thus, we can determine which patients have the activated receptor and provide evidence that P-IGF-IR/IR is a prognostic factor for breast cancer. Beyond this, P-IGF-IR/IR could be a predictive marker for response to IGF-IR and/or IR-targeted therapies, as these inhibitors may be of benefit in all breast cancer subtypes including those with acquired resistance to tamoxifen.

Introduction

The insulin-like growth factor-I receptor (IGF-IR) has become an attractive molecular target for cancer treatment given as it is expressed in a wide range of tumors including those that arise in the breast. Several studies indicate that IGF-IR activation is associated with the growth, invasion, and metastasis of breast cancer (1) and where estrogen receptor (ER) is present, also interplays with this steroid hormone receptor to promote growth (2). The expression of constitutively active IGF-IR in the mammary gland leads to the development of tumors (3) while overexpression of a constitutively activated IGF-IR (CD8-IGF-IR) is sufficient to cause transformation of immortalized human mammary epithelial cells and growth in immunocompromised mice (4). Conversely, silencing IGF-IR with small molecules inhibits the growth of mammary cells (IGF-IR-Sal) expressing constitutively activated IGF-IR in a xenograft model (3). As well, IGF-IR neutralizing antibodies suppress the growth of breast cancer cells implanted as xenografts (5). Furthermore, transgenic mice that express activated IGF-IR in the mammary gland under a doxycycline inducible promoter developed tumors at 2 months of age (6). Thus, IGF-IR signaling is important for the development of breast tumors and cancers continue to depend upon this pathway for sustained growth and survival.

Given the importance of IGF-IR in tumor growth, it has become an attractive molecular target for therapy and small molecules as well as antibodies are being developed to inhibit this pathway (7–10). Although most of them are directed against IGF-IR, some also inhibit insulin receptors (IR), which could be additionally beneficial given that IGF-IR and IR form heterodimers (11, 12) and that the IR itself has been shown to be important in cancers (13). For example, two recent dual specificity inhibitors, BMS-554417 and BMS-536924, were found to target both the IGF-IR and IR and were active *in vivo* (4, 14, 15). Although these compounds can lead to hyperglycemia, there is recent preclinical evidence that this adverse effect can be attenuated by the use of metformin.[5]

The IGF-IR pathway is also implicated in resistance to targeted therapies including those that target the ER and the epidermal growth factor receptor (EGFR) family members EGFR and HER2. For example, IGF-IR is reportedly up-regulated during the acquisition of tamoxifen resistance. The continuous exposure of MCF-7 cells to tamoxifen resulted in the eventual emergence of resistant cells, called MCF-7 Tam-R, which use IGF-IR for their growth (16, 17). Activation of the IGF-IR signaling cascade has also been reported in models of resistance to agents that target

[5] J. Carboni, unpublished data.

the EGFR family (16, 18–20). It is therefore rational to inhibit the IGF-IR pathway to prevent or attenuate the development of resistance (21) and to use IGF-IR inhibitors in circumstances where acquired resistance has developed over time.

Understanding the clinical role of IGF-IR/IR signaling in different subtypes of breast cancer is also very important in the treatment of patients because each subtype has a clinically distinct outcome and therefore requires a different treatment protocol. ER-positive luminal breast cancers usually have better outcomes compared with the aggressive ER-negative, HER2, and triple-negative groups (22). Tamoxifen or aromatase inhibitors are generally the first line therapy for luminal patients, whereas trastuzumab is prescribed for HER2 overexpressing breast cancer patients. Unfortunately, there is currently no targeted treatment for triple-negative breast cancers. These tumors do not express ER, progesterone receptor (PR), nor do they overexpress HER2, and 65–80% of patients usually die within two years of diagnosis (23, 24). The relative importance of IGF-IR/IR signaling in different types of breast cancer is still unclear.

Previously, we have shown that total IGF-IR expression in breast cancer was evident in 87% of primary breast tumors by screening a cohort of 930 patient samples (25). At that time, we were unable to determine whether or not the receptor was activated because suitable antibodies were not available, although a subsequent small study indicated that activation of IGF-IR is detectable in clinical disease (26). Given the growing interest in IGF-IR as a target for cancer therapy (27), and the development of several new drug candidates against IGF-IR (28), it is timely that we now evaluate the role of activated IGF-IR/IR in the large series of primary breast tumors in relation to patient survival as well as the potential application of IGF-IR/IR inhibitors in key subtypes of this disease.

In this study, we report that activated IGF-IR/IR is predicative of poor outcomes for breast cancer patients after screening 438 primary tumor tissues. We further show that the downstream protein phospho-S6 was correlated with P-IGF-IR/IR expression in these clinical specimens. Using MCF-7 (as a model ER-positive luminal breast cancer), SUM149 (as a model for ER-negative triple-negative breast cancer), and AU565 (representing HER2 overexpressing breast cancer) cell lines, we also show that the small molecule IGF-IR tyrosine kinase (TK) inhibitor, BMS-536924 (10), actively inhibited growth of all cell lines, including a tamoxifen resistance MCF-7 subtype, in two-dimensional (collagen matrix) and three-dimensional (soft agar) culture systems.

Materials and Methods

Clinical breast cancer tissue microarray construction. The tissue microarray (TMA) was composed of duplicate cores from 438 primary breast tumors. Construction of the TMA and the clinical correlates were previously described by us (29–31).

Optimization of phospho-IGF-IR/IR staining. Previous studies by this group (JG, HJ, RN) showed that IGF-IR is highly expressed and activated in DU145 prostate cancer cells that had acquired resistance to gefitinib (DU145/TKIR; ref. 16). This activity is reversible using IGF-IR TK inhibitors such as AG1024 (16). To ensure specificity of staining obtained with the phospho-IGF-IR (Tyr1131)/IR (Tyr1146; Cell Signaling Technologies #3021) antibody to be used for the current clinical studies, we first evaluated this antibody within the DU145/TKIR cells. These cells were maintained in DCCM-1 medium containing 1 μmol/L gefitinib and plated at 7.5×10^3 cells/22 mm^2 coverslip and grown to 60% confluence as previously described (16). The DU145/TKIR cells were then treated with or without 20 μmol/L of the IGF-IR–selective TK inhibitor AG1024 for 24 h (16). The cells were immunostained on coverslips for phosphorylated IGF-IR/IR using the above antibody or evaluated by immunoblotting, as previously described (16). P-IGF-IR/IR staining was detected as a crisp plasma membrane signal in the DU145/TKIR cells while treating with 20 μmol/L AG1024 depleted this staining (Supplementary Fig. S1*A*). Findings were corroborated by an equivalent profile by Western blot analysis with this antibody (Supplementary Fig. S1*B*). Sections (5 μm) of formalin-fixed/paraffin-embedded DU145/TKIR cell pellets were subsequently stained using this antibody as applied in the clinical assay procedure (see below). Again, the DU145/TKIR cells stained at the plasma membranes, whereas there was no staining was seen in R-(IGF-IR-null) fibroblast paraffin-embedded pellets (a kind gift from V. Macaulay, Weatherall Institute of Molecular Medicine, Oxford, United Kingdom and R. Baserga Kimmel Cancer Centre, Philadelphia; ref. 32), further confirming appropriate antibody performance for the clinical assays (Supplementary Fig. S1*C*) and providing appropriate positive and negative assay controls, respectively.

P-IGF-IR/IR staining. After initial antibody verification as described above, primary breast tumors were stained with the P-IGF-IR/IR antibody in the formalin-fixed paraffin embedded TMAs. Initially the 5-μm sections from the TMA had endogenous peroxidases blocked with 3% hydrogen peroxide for 5 min. Antigen retrieval was performed by heating the slides in a pressure cooker in EDTA buffer (pH 8) followed by cooling for 10 min in gently running tap water. The slides were then blocked in 0.02% Tween/PBS for 5 min and incubated in P-IGF-IR/IR antibody (diluted 1:20 in PBS) overnight at 23°C. After 3 washes in PBS, rabbit EnVision peroxidase-labeled polymer antibody (Dako; #K4011) was applied for 2 h at 23°C. The slides were developed with 3,3′-diaminobenzidine (DAB)/H_2O_2 chromagen for 8 min and counterstained with hematoxylin (EMD Chemicals, Inc.). Internal positive and negative control slides for the TMA assay comprised 5-μm sections of the formalin-fixed/paraffin embedded DU145/TKIR cell pellets and R-(IGF-IR-null) fibroblast pellets, respectively. Tumors showing no staining were considered P-IGF-IR/IR negative, whereas plasma membranous weak, moderate, or strong staining was considered positive.

Phospho-S6 ribosomal protein staining. To assess ribosomal P-S6, the TMA slides were incubated at 60°C before deparaffinization and rehydration. Antigen retrieval was performed by heating the slides in citrate buffer at 98°C for 30 min. After cooling and washing with PBS, endogenous peroxidases were blocked with 3% hydrogen peroxide for 10 min. The slides were blocked with DAKO protein block (Dako Cytomation Protein Block Serum-Free) and stained with rabbit polyclonal P-S6 ribosomal antibody (Cell Signaling; Ser235/236) at a dilution of 1:200 overnight at 4°C. After a PBS wash (3 min), followed by two 0.02% Tween/PBS washes, the secondary antibody was applied directly to the slides [Dako Cytomation Envision R system; anti-rabbit horseradish peroxidase HRP] for 30 min. The arrays were then washed with PBS/Tween 20 (0.1%) and stained with Nova Red (Vector NovaRED substrate kit from Vector laboratories) for 1 min and counterstained with Hematoxylin for 30 s. Specimens with no staining were considered negative for P-S6, and those with any level of cytoplasmic staining were considered positive.

Immunohistochemistry for IGF-IR, IR, and other markers. Total IGF-IR staining and scoring was performed according to Nielsen and colleagues (25). For total IR, following dewaxing and rehydration, endogenous peroxidases were blocked using 3% hydrogen peroxide (5 min). Antigen retrieval was performed by pressure-cooking in sodium citrate buffer (pH 6) for 2 min. After cooling for 10 min in gently running tap water, slides were washed in PBS and blocked with 0.02% Tween/PBS for 5 min. The IR antibody was applied at (60 μL of 4 μg/mL in PBS) to each section overnight at room temperature (#GR36 Calbiochem mouse anti-human IR-β-subunit). After one wash in PBS (3 min), followed by two 0.02% Tween/PBS washes, the secondary antibody (mouse EnVision peroxidase labeled polymer antibody) was applied for 1.5 h at room temperature. The slides were again washed as above, and then an EnVision DAB chromagen was applied to sections for 10 min. Aqueous methyl green (0.5%) was used as a

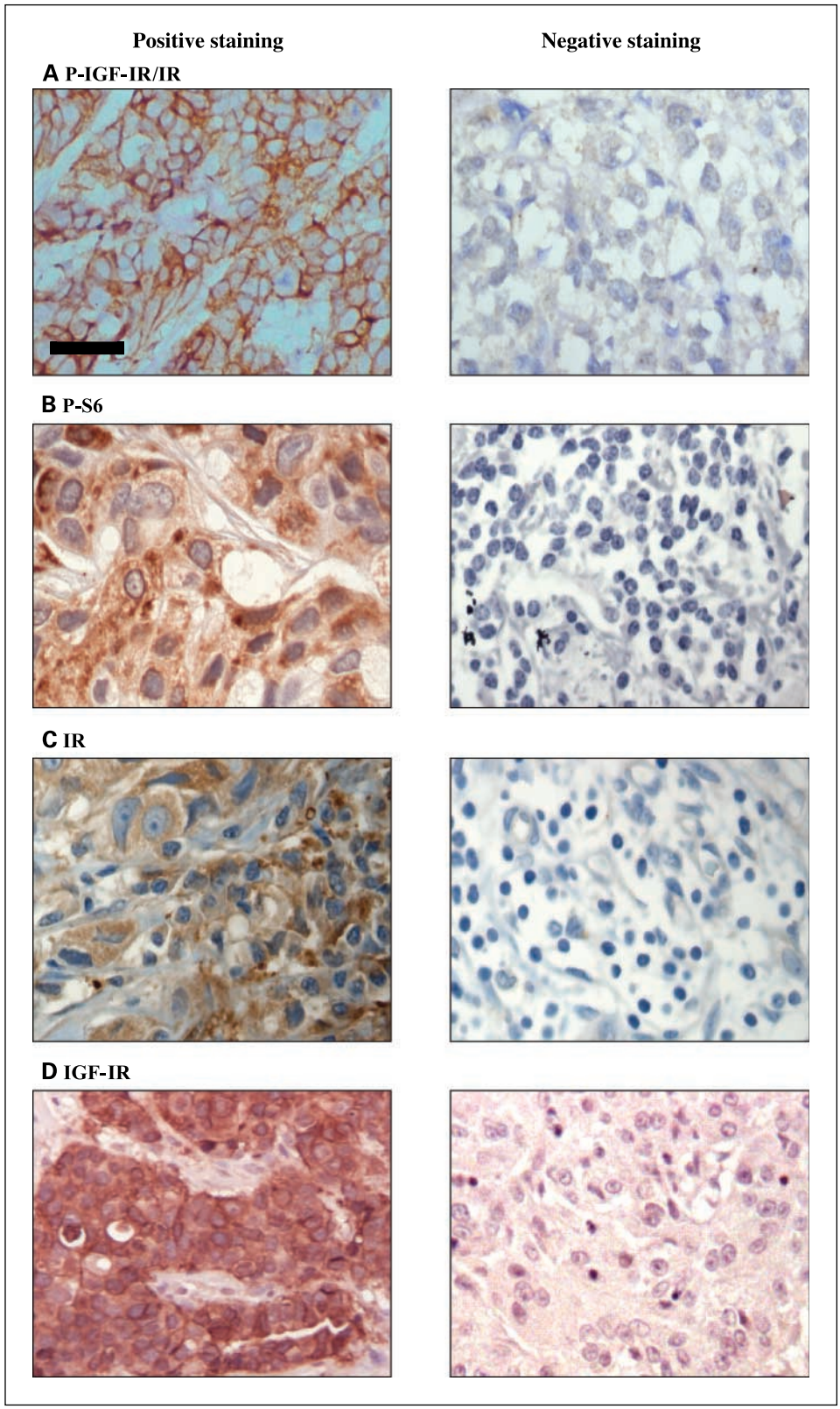

Figure 1. Representative panel of immunohistochemical stainings on primary breast tumors. Examples of positive (*right*) and negative (*left*) immunostaining TMA cores for (*A*) phospho-IGF-IR/IR antibody, (*B*) phospho-S6 ribosomal protein antibody, (*C*) total IR antibody, and (*D*) total-IGF-IR antibody. *Bar,* 25 μm.

counterstain. Tumors showing no staining were considered IR negative, and those with weak, moderate, or strong membranous and cytoplasmic staining were considered IR positive.

P-Akt^{S473} and ER staining, localization, and scoring have been described previously by us (29–31). Ki67 (mouse monoclonal clone K-2; Ventana Medical Systems) staining was performed on a Ventana machine using a standard CC1 antigen retrieval followed by a 16 min primary incubation with heat. Detection was carried out with the DABMap kit (Ventana). Nuclear staining of <10% was categorized as negative, whereas tumors with >10% nuclear staining were considered positive.

Statistical analysis of the TMA data. Correlations between P-IGF-IR/IR, IR, IGF-IR, P-S6$^{S235/236}$, P-Akt^{S473}, Ki67, and ER staining in the clinical samples were determined using a Spearman's test (SPSS software, version 13). Patient survival was determined using Breslow univariate statistical analysis and Kaplan-Meier curves. Patients who were missing diagnostic or survival information were excluded from analysis. Results were considered statistically significant with a P value of <0.05.

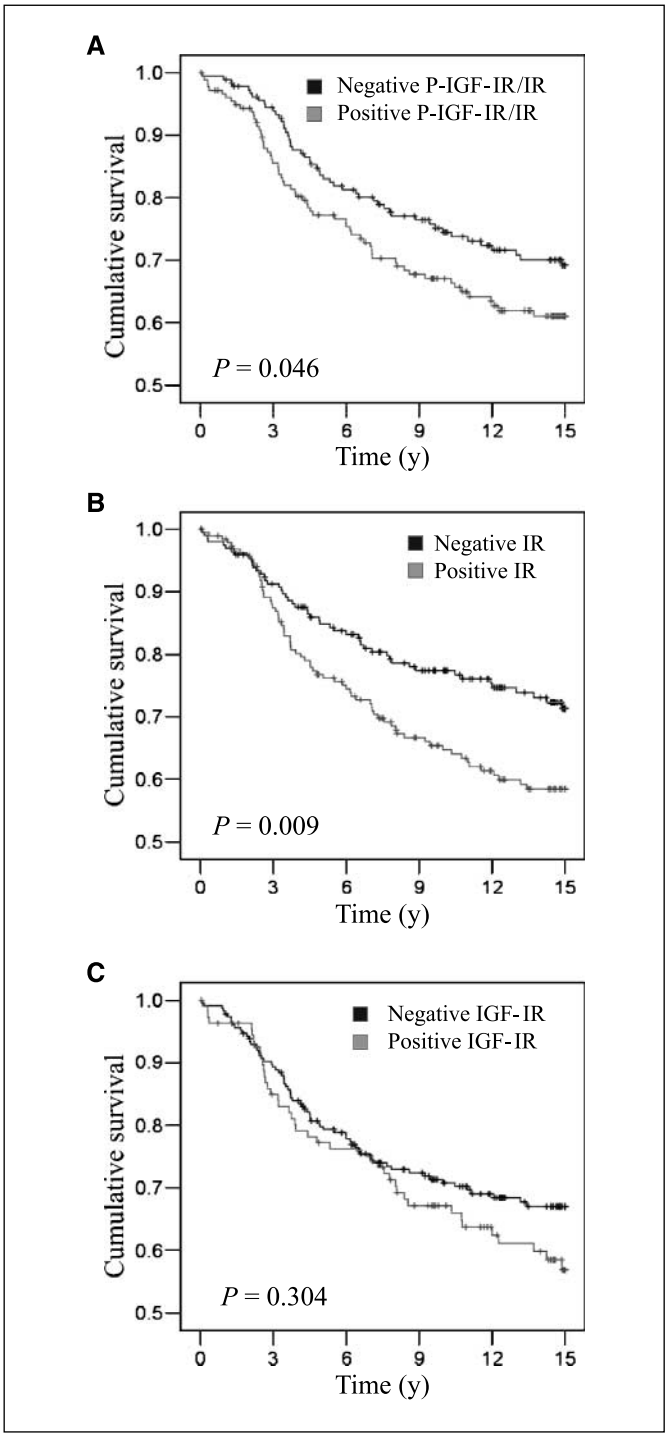

Figure 2. Breast cancer specific survival analysis at 15 y. *A,* P-IGF-IR/IR expression (n = 114; 55.3% positive, 44.7% negative) and (*B*) total IR expression (n = 122; 59.0% positive, 41.0% negative) are correlated with poor outcome, whereas (*C*) total IGF-IR expression (n = 112; 37.5% positive, 62.5% negative) in primary breast tumors is not associated with shorter survival time based on Kaplan Meier survival analyses.

Models of breast cancer subtypes and BMS-536924. Hormone-responsive parental MCF-7 and the tamoxifen-resistant subline MCF-7 Tam-R were routinely grown in 10% fetal bovine serum (FBS) phenol red–free RPMI (Life Technologies/Invitrogen). Tam-R cells were grown with the addition of 100 nmol/L 4-OH-tamoxifen (Sigma) to sustain resistance. Cell culture for the triple-negative breast cancer model SUM149 cells (Astrand) was as previously described (33). AU565 cells (American Type Culture Collection), our model of HER2 overexpressing breast cancer cells, were cultured in 10% FBS RPMI (Life Technologies/Invitrogen). HTRY cells were immortalized human breast epithelial cells developed from HMEC cells at Wake Forest University, USA (34), and were grown in the same medium as SUM149. Human telomerase–immortalized breast epithelial (184htrt) cells were grown as previously described (35). All cell lines were grown at 37°C with 5% CO_2. BMS-536924, a small molecule TK inhibitor of IGF-IR, was kindly supplied by Bristol Myers Squibb. The drug was dissolved in DMSO and stored at −20°C until use.

Immunoblotting. MCF-7, SUM149, AU565, MCF-7 Tam-R, and HTRY cells were seeded at 5×10^5 cells in 6-well plates containing complete medium. Cells were serum starved for 24 h then treated with either DMSO or 4 μmol/L BMS-536924 for 1 h followed by IGF-I stimulation for 15 min. Cells were lysed as previously described (36) and proteins were evaluated by immunoblotting. Membranes were blocked with 5% bovine serum albumin in TBS-T for 1 h then incubated with Phospho-IGF-IR β (Tyr1135/1136)/IR β (Tyr1150/1151) antibody (Cell Signaling #3024) overnight at 4°C. Rabbit HRP secondary antibody (Cell Signaling) was used and membranes were visualized with Amersham ECL Western Detection Kit (GE Healthcare) on X-ray film. Membranes were also immunoblotted for P-S6$^{S235/236}$, total IGF-IR (Santa Cruz #713), phospho-p90RSK^{S380} (Cell Signaling #9340), and total RSK (Cell Signaling #9347). Actin (Cell Signaling #4968) was used as a loading control.

***In vitro* proliferation assay of the IGF-IR inhibitor.** Cells (MCF-7, MCF-7 Tam-R, SUM149, AU565, and HTRY) were seeded in 96-well plates (collagen I coated; BD) at 5,000 cells per well in 100 μL of appropriate medium. Collagen-coated plates were used as they best represent of the epithelial-stromal environment that breast cancer cells normally encounter. Collagen I was selected because it constitutes one of the most abundant extracellular matrix proteins in the breast (37). BMS-536924 was diluted in medium and added accordingly to each well 24 h postseeding to give final concentrations of 0 (DMSO only), 0.5, 1.0, 2.0, or 4.0 μmol/L. There were four replicate wells for each treatment and the experiments were repeated in triplicate. MCF-7 and MCF-7 Tam-R cells were also treated with BMS-536924 in serum-free (SF) medium containing IGF-I (100 ng/mL) or IGF-I plus estradiol (10 nmol/L; Sigma). After 72 h of drug treatment, medium was aspirated and the cells fixed and stained with 100 μL of 2% paraformaldehyde (Sigma) with 1 μg/mL Hoechst (Sigma) for 30 min. After washing once with PBS, cells were stored in PBS at 4°C. The plates were analyzed on a high-content screening instrument, the ArrayScan Reader (Cellomics). Twenty fields were counted for each replicate well and the results were presented as an average ± SD.

Soft agar assays. MCF-7 and MCF-7 Tam-R cells were plated at 2.5×10^4 cells per well of a 6-well plate, whereas SUM149 (1×10^4) and AU565 (5×10^3) were plated in a 24-well plate in 0.6% soft agar as previously described (30). BMS-536924 was added at the time of seeding to the cell layer (DMSO control, 0.5, 1.0, and 2.0 μmol/L). Colonies were counted after 28 to 30 d. Each treatment was performed in triplicate on two separate occasions.

Results

P-IGF-IR/IR and IR are associated with poor outcome. In this cohort of 438 patients, tumors were immunostained for P-IGF-IR/IR, P-S6, IGF-IR, and IR (representative images, Fig. 1*A–D*). P-IGF-IR/IR was detected in 49.3% of tumors (178 of 361 scorable cases), whereas P-S6 was present in 56.6% (172 of 304), IGF-IR in 32.4% (110 of 339), and IR in 48.8% (188 of

Table 1. Evaluation of P-IGF-IR/IR with other markers in primary breast tumors

Marker	Spearman's correlation	*P*	*N*
P-S6$^{S235/236}$	0.208	6.544×10^{-4}	266
P-Akt^{S473}	0.090	0.104	329
Ki67	0.130	0.018	335
ER	−0.057	0.348	271
IR	0.064	0.239	342
IGF-IR	0.048	0.410	295

NOTE: P-IGF-IR/IR was correlated with P-S6 and Ki67 yet not with other proteins.

385) of cases. Positive P-IGF-IR/IR immunostaining was associated with poor survival when assessed at 15 years (n = 114; 55.3% positive; 44.7% negative; Breslow P = 0.046; Fig. 2*A*). Total IR expression in this cohort was also associated with poor survival (n = 122; 59.0% positive, 41.0% negative; Breslow P = 0.009; Fig. 2*B*), whereas IGF-IR was not (n = 112; 37.5% positive, 62.5% negative; Breslow P = 0.304; Fig. 2*C*).

P-IGF-IR/IR is positively correlated with P-S6. To understand what signaling pathway may be affected, we immunostained for P-Akt and P-S6, both of which are activated by IGF-I and insulin *in vitro*. Activated IGF-IR/IR was directly correlated with expression of P-S6, with 68% of cases having detectable levels of both (likelihood ratio, 11.57; $P = 6.70 \times 10^{-4}$). P-IGF-IR/IR was also significantly correlated with Ki67 (P = 0.018) but not with P-Akt, ER, IR, or IGF-IR (Table 1). It seemed that P-Akt (P = 0.104; Table 1) was a less reliable indicator of P-IGF-IR/IR, suggesting that P-S6 ($P = 6.54 \times 10^{-4}$; Table 1) is a better sentinel marker for these receptors, although there was a weak positive correlation between P-S6 and P-Akt (Spearman's Correlation, 0.102; P = 0.085). There was also no correlation with the ER (Table 1), suggesting that P-IGF-IR/IR–targeted inhibitors may benefit patients independent of their hormone receptor status.

P-IGF-IR/IR spans all breast cancer subtypes. Because P-IGF-IR/IR was not correlated with ER, we looked at its distribution throughout this cohort. Importantly, P-IGF-IR/IR was expressed in all breast cancer subtypes (Fig. 3*A*), implying that it may represent a therapeutic target with broad relevance in this disease. In our series, the luminal subtype comprises the largest proportion of breast cancers (n = 181 of 226), followed by the triple negative (n = 31 of 226), and HER2 overexpressing (n = 14 of 226) subtypes. We found that P-IGF-IR is detectable in about half of all breast cancers regardless of subtype, with luminal having 48.1% expression (n = 87 of 181), triple negative having 41.9% (n = 13 of 31), and HER2 overexpressing with 64.3% (n = 9 of 14). Furthermore, we determined that P-IGF-IR/IR was not specific to a particular subtype (likelihood ratio, 1.96; P = 0.38).

BMS-536924 suppresses the growth of breast cancer subtypes *in vitro*. The TMA findings prompted us to evaluate the potential of IGF-IR/IR inhibition *in vitro* using MCF-7, SUM149, and AU565 cell lines, as representatives of luminal, triple-negative, and HER2 overexpressing breast cancers, respectively. Each cell line showed activated P-IGF-IR/IR in the presence of IGF-I, and in each case receptor activation was inhibited by BMS-536924 (Fig. 3*B*). We observed a concomitant reduction in P-S6 in MCF-7 and SUM149 cells but not in AU565 cells. Because P-IGF-IR/IR was not correlated with P-Akt in the TMA, we queried if the effect on P-S6 could be through an alternative pathway such as RSK. Indeed, we found that in all cancer cell lines, P-RSK decreased with BMS-536924 drug treatment (SUM149 > MCF7 > AU565; Fig. 3*B*).

The drug suppressed growth of MCF-7 cells in a dose-dependent manner from 0 to 4 μmol/L (Fig. 4*A, left*). We also showed that BMS-536924 inhibited the growth of MCF-7 cells when stimulated with either IGF-I or IGF-I/estradiol. Consistent with this finding, BMS-536924 had a robust inhibitory effect on the growth of the MCF-7 cells in soft agar (Fig. 4*A, right*). SUM149 cells were also sensitive to inhibition of P-IGF-IR with BMS-536924 in both monolayer (Fig. 4*B, left*) and soft agar (Fig. 4*B, right*) in a dose-dependent manner. AU565 showed a decrease in growth (Fig. 4*C, left* and *right*) with addition of BMS-536924; however, it was not as striking as the inhibition seen in MCF-7 or SUM149

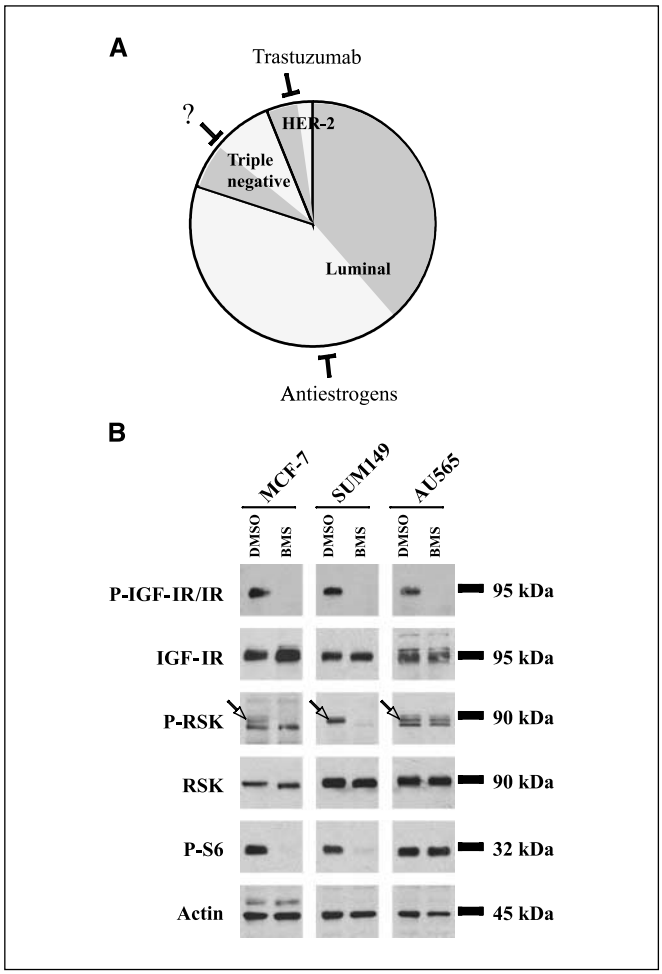

Figure 3. *A,* schematic showing the relative incidence of breast cancer subtypes in the TMA. Luminal (ER+), n = 181; triple-negative (ER−, HER2−, PR−), n = 31; HER2 (ER−, HER2+), n = 14. Activated IGF-IR/IR is expressed in all breast cancer subtypes as shown by the shaded areas in each subtype and with the following percentages: luminal, 48.1% (n = 87 of 181); triple-negative, 41.9% (n = 13 of 31); HER2, 64.3% (n = 9 of 14; likelihood ratio, 1.96; P = 0.38). Current targeted therapies for each subtype are indicated. *B,* evaluation of P-IGF-IR/IR, P-RSK (*top band, arrow*), and P-S6 in MCF-7 (luminal), SUM149 (triple negative), and AU565 (HER2 overexpressing) cells. Cells were treated with DMSO or BMS-536924 (4 μmol/L) for 1 h followed by IGF-I stimulation (100 ng/mL for 15 min). Loading control is actin.

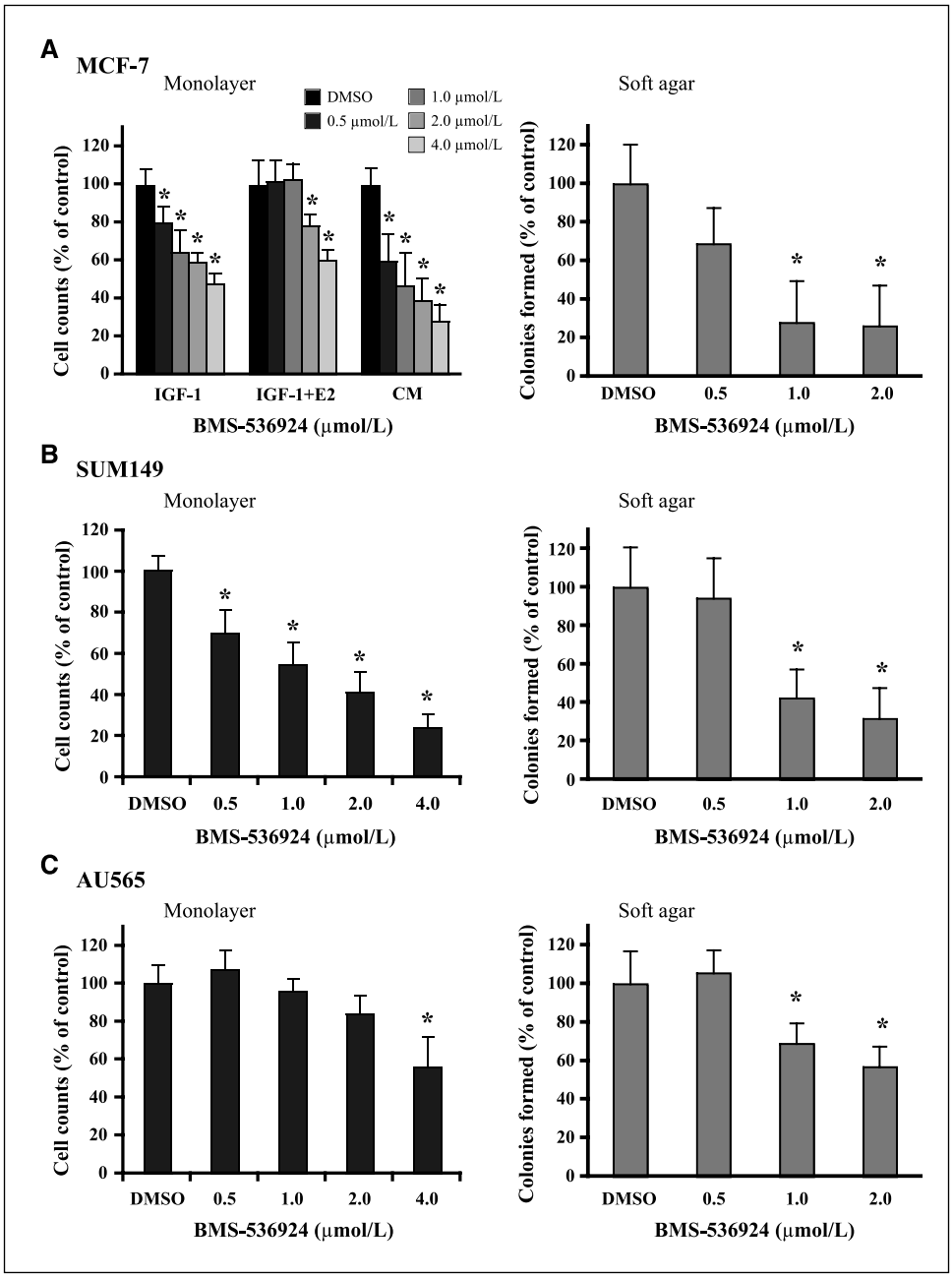

Figure 4. BMS-536924 inhibits growth in all breast cancer subtype cell lines in both monolayer (*left*) and soft agar (*right*). In monolayer (*left*), (*A*) MCF-7 cells, (*B*) SUM149 cells, and (*C*) AU565 cells were treated with DMSO or 0.5 to 4 μmol/L BMS-536924 for 72 h, followed by Hoechst staining and cell counting. MCF-7 cells were also treated in SF medium containing IGF-I (100 ng/mL) or IGF-I plus estradiol (E2; 10 nmol/L). *CM,* complete media. For soft agar assays (*right*), DMSO or BMS-536924 (0.5–2 μmol/L) was added at the time of seeding to the cell layer. Colonies were counted after 28 to 30 d. In all cases, treatments were compared with DMSO control; *, $P < 0.001$.

cells. To address the possibility that IGF-IR/IR inhibition would be valuable in situations where tumor cells have acquired drug resistance, we also studied the tamoxifen-resistant MCF-7 Tam-R cell model. We observed that MCF-7 Tam-R cells express activated IGF-IR/IR and that activation can be blocked by the addition of BMS-536924 (Fig. 5*A*). As in the other breast cancer cells tested, this drug inhibited the growth of MCF-7 Tam-R cells in monolayer (Fig. 5*B, top*) as well as in soft agar (Fig. 5*B, bottom*), implying that these tamoxifen-resistant cells require IGF-IR/IR for their growth and survival. Finally, we evaluated the effects of BMS-536924 in the normal breast epithelial models, HTRY and 184htrt cells. Although this drug blocked signaling in the HTRY cells (Fig. 5*C*), the drug did not significantly inhibit on growth in monolayer (Fig. 5*D*). A similar trend was also observed in 184htrt cells (data not shown).

Discussion

In this study, we found that P-IGF-IR/IR is detectable in tumors of all breast cancer subtypes and is associated with increased probability of breast cancer–related deaths. We also observed a strong correlation between P-IGF-IR/IR and P-S6 in primary tumors, suggesting that the latter maybe be a useful downstream marker for activation or inhibition of this pathway. As such, P-S6 staining was reportedly used as a predictive marker for agents targeting mammalian target of rapamycin in sarcomas (38). More importantly, we observed no correlation between total IR or total IGF-IR and P-IGF-IR/IR or P-S6, further upholding the prognostic value of P-S6 as specific marker for IGF-I receptor activation in primary tumors. Monitoring P-S6 down-regulation, as we did with BMS-536924 where this surrogate marker was suppressed in three

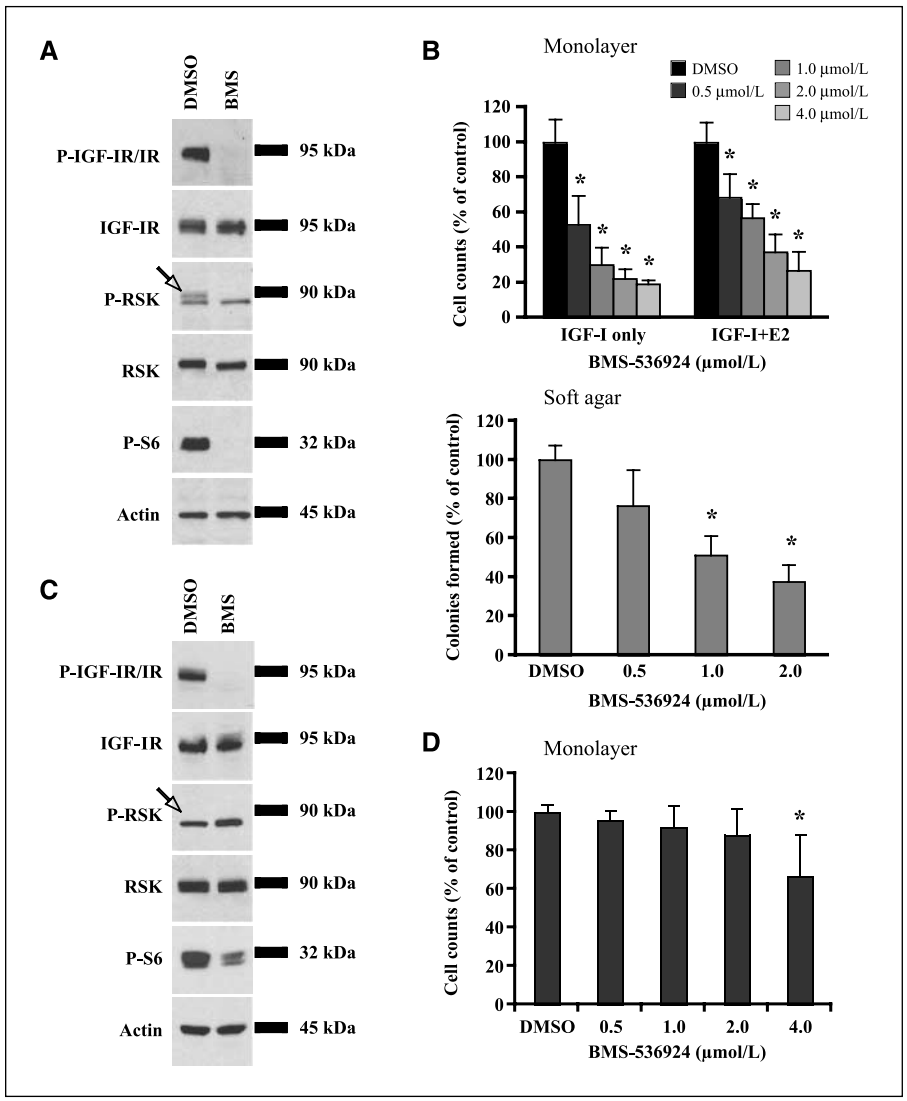

Figure 5. BMS-536924 inhibits cell growth in tamoxifen-resistant cells, MCF-7 Tam-R cells. *A,* Western blot showing that BMS-536924 decreases P-IGF-IR/IR, P-RSK (*top band, arrow*) and downstream P-S6 in MCF-7 Tam-R cells. Cells were treated with DMSO or BMS-536924 (4 μmol/L) for 1 h followed by IGF-I stimulation (100 ng/mL for 15 min). Loading control is actin. *B,* BMS-536924 inhibits growth in both monolayer (*top*) and soft agar (*bottom*) in MCF-7 Tam-R cells. In monolayer, cells were treated with DMSO or 0.5 to 4 μmol/L BMS-536924 for 72 h, followed by Hoechst staining and cell counting. In soft agar, DMSO or BMS-536924 (0.5–2 μmol/L) was added at the time of seeding to the cell layer and colonies were counted after 28 to 30 d. BMS-536924 does not profoundly reduce growth in HTRY cells. *C,* HTRY (immortalized human breast epithelial) cells show a complete reduction in P-IGF-IR, whereas P-S6 is only slightly decreased with BMS-536924 treatment. P-RSK was not observed in these cells, as there is no top band by Western (*arrow*). *D,* the drug does not significantly perturb HTRY growth in monolayer after 72 h. Treatment conditions were as above. *, $P < 0.001$.

of four cell lines, may therefore be useful in determining response to IGF-IR inhibitors.

Because we observed no correlation of P-IGF-IR/IR with P-Akt in the clinical specimens, we were curious if *in vitro* the decrease in P-S6 could be linked to an alternate signaling route. The serine threonine kinase RSK is downstream of mitogen-activated protein kinase (MAPK) and extracellular signal-regulated kinase, and does not rely on signaling through Akt (39). Although RSK is relatively unknown in the breast cancer field, it has the same recognition sequence as Akt, binding to substrates with RxRxxS motifs (40). Thus, we probed for activation of RSK and show that P-RSK is decreased with BMS-536924 treatment in MCF-7, SUM149, and AU565 cells. Although AU565 cells showed only a partial suppression of P-RSK, this may be because they also express amplified HER2, which activates the phosphatidylinositol-3-OH kinase and MAPK pathways and, subsequently, P-S6. Recent evidence demonstrating that HER signaling confers resistance to BMS-536924 (41) supports this conclusion. To our knowledge, there is only one other study showing that RSK may have a role in breast cancer (42). Thus, the discovery that inhibition of IGF-IR/IR causes a decrease in P-RSK, and therefore, inactivation of P-S6 is novel and brings new insight into the mechanism of action of BMS-536924.

In contrast to studies showing that total IGF-IR protein expression is correlated with ER in breast cancer tumors (12), we find that P-IGF-IR/IR is not correlated with this steroid hormone receptor. This result was also suggested in early studies with a different phospho-IGF-IR antibody (26) in a small (n = 64) historical, paraffin-embedded, primary breast cancer series. In fact, we show that P-IGF-IR/IR has an equal distribution across all breast tumor subtypes and is found in about half of all specimens independent of ER status. Taken together with our data showing that P-IGF-IR/IR expression is correlated with poor outcome, whereas total IGF-IR is not, we therefore suggest that activated IGF-IR is more indicative of disease biology than total IGF-IR level. This observation may also explain why other groups report differing prognosis based on total IGF-IR versus ER status (12).

The IGF-IR/IR family is complex, with structural homology between IGF-IR and IR, allowing the formation of hybrid receptors consisting of an IGF-IR αβ-chain complexed with an IR αβ-chain (11, 12, 43). Because immunohistochemistry cannot distinguish

between the holoreceptor and hybrid receptors, we interpret positive staining with P-IGF-IR/IR, IGF-IR, and IR antibodies as evidence for either or both types of receptors. Although our results provide new evidence for the relation of IGF-IR/IR family members to clinical outcome, we cannot address the issue of relative importance of activation of IGF-I, insulin, or hybrid receptors. Importantly, the observation that P-IGF-IR/IR is related to outcome whereas IGF-IR is not is consistent with the notion that, unlike HER2-neu, IGF-IR/IR is not constitutively active in cancers rather depend upon ligand binding. Furthermore, the observation that IR is correlated with poor survival in this cohort is of interest in the context that high levels of insulin have been associated with adverse outcome in breast cancer patients and in various tumor models (13). Additional work is needed to evaluate the clinical relevance of this finding.

Because P-IGF-IR/IR is expressed in all subtypes of breast cancer, we assessed the effect of BMS-536924 in *in vitro* models of each. Treating both ER-positive MCF-7 cells and ER-negative SUM149 and AU565 cells with this inhibitor resulted in suppression of cancer cell growth in a dose-dependent manner, although AU565 cells, which overexpress HER2, were not as sensitive to BMS-536924. We also do not see a corresponding decrease in P-S6 in the AU565 cells, likely due to HER2 being the dominant receptor TK for these cells when it is not therapeutically blocked. These results are consistent with the studies of Chakraborty and colleagues (44), in which they observed cross-talk between IGF-IR and HER2 and a synergistic growth suppression that was achieved only by combining inhibitors to both receptors.

The significant growth inhibition in the triple-negative breast cancer model, SUM149, is noteworthy as it raises the possibility that at least a subset of these aggressive cancers may be inhibited by targeting IGF-IR/IR. Furthermore, the evidence that BMS-536924 inhibits growth of MCF-7 Tam-R cells suggests that blocking IGF-IR signaling may also benefit those with acquired tamoxifen resistance. Our finding that activation of IGF-IR is important in both tamoxifen-responsive and tamoxifen-resistant breast cancer cell models is complemented by the preliminary clinical study reported from Gee and colleagues (26) who showed, using an alternative phospho-IGF-IR antibody, that immunostaining is readily detectable in tamoxifen-responsive, *de novo* tamoxifen-resistant, and also acquired tamoxifen-resistant clinical breast cancer samples. We also show that although BMS-536924 can block signaling in HTRY cells, it does not greatly effect growth in these normal breast epithelial cells, suggesting that this pathway is not critical for survival in normal cells.

The importance of the IGF-IR pathway for the growth of many types of cancer including breast has led to the development of inhibitors directed against this target and several on-going clinical trials (8, 9). We show for the first time that P-IGF-IR/IR is associated with poor survival in breast cancer, and thus, it may be used as a candidate prognostic biomarker. Furthermore, identification of tumors with activated IGF-IR/IR may allow selection of patients that will benefit from individualized therapies that inhibit this pathway. We also provide evidence that the IGF-IR/IR inhibitor BMS-536924 shows preclinical activity in all breast cancer subtypes and in a model of acquired resistance to antiestrogens. These findings raise the possibility that IGF-IR/IR inhibition may be broadly useful in treatment of all breast cancers, and justify clinical research.

Disclosure of Potential Conflicts of Interest

No potential conflicts of interest were disclosed.

References

1. Kucab JE, Dunn SE. Role of IGF-1R in mediating breast cancer invasion and metastasis. Breast Dis 2003;17:41–7.
2. Dupont J, Le Roith D. Insulin-like growth factor 1 and oestradiol promote cell proliferation of MCF-7 breast cancer cells: new insights into their synergistic effects. Mol Pathol 2001;54:149–54.
3. Carboni JM, Lee AV, Hadsell DL, et al. Tumor development by transgenic expression of a constitutively active insulin-like growth factor I receptor. Cancer Res 2005;65:3781–7.
4. Kim HJ, Litzenburger BC, Cui X, et al. Constitutively active type I insulin-like growth factor receptor causes transformation and xenograft growth of immortalized mammary epithelial cells and is accompanied by an epithelial-to-mesenchymal transition mediated by NF-κB and snail. Mol Cell Biol 2007;27:3165–75.
5. Arteaga CL, Kitten LJ, Coronado EB, et al. Blockade of the type I somatomedin receptor inhibits growth of human breast cancer cells in athymic mice. J Clin Invest 1989;84:1418–23.
6. Jones RA, Campbell CI, Gunther EJ, et al. Transgenic overexpression of IGF-IR disrupts mammary ductal morphogenesis and induces tumor formation. Oncogene 2007;26:1636–44.
7. Zhang H, Yee D. The therapeutic potential of agents targeting the type I insulin-like growth factor receptor. Expert Opin Investig Drugs 2004;13:1569–77.
8. Tao Y, Pinzi V, Bourhis J, Deutsch E. Mechanisms of disease: signaling of the insulin-like growth factor 1 receptor pathway-therapeutic perspectives in cancer. Nat Clin Pract Oncol 2007;4:591–602.
9. Ryan PD, Goss PE. The emerging role of the insulin-like growth factor pathway as a therapeutic target in cancer. Oncologist 2008;13:16–24.
10. Wittman M, Carboni J, Attar R, et al. Discovery of a (1H-benzoimidazol-2-yl)-1H-pyridin-2-one (BMS-536924) inhibitor of insulin-like growth factor I receptor kinase with *in vivo* antitumor activity. J Med Chem 2005; 48:5639–43.
11. Dupont J, Dunn SE, Barrett JC, LeRoith D. Microarray analysis and identification of novel molecules involved in insulin-like growth factor-1 receptor signaling and gene expression. Recent Prog Horm Res 2003;58:325–42.
12. Hartog H, Wesseling J, Boezen HM, van der Graaf WT. The insulin-like growth factor 1 receptor in cancer: old focus, new future. Eur J Cancer 2007;43:1895–904.
13. Frasca F, Pandini G, Sciacca L, et al. The role of insulin receptors and IGF-I receptors in cancer and other diseases. Arch Physiol Biochem 2008;114:23–37.
14. Hofmann F, Garcia-Echeverria C. Blocking the insulin-like growth factor-I receptor as a strategy for targeting cancer. Drug Discov Today 2005;10:1041–7.
15. Haluska P, Carboni JM, Loegering DA, et al. *In vitro* and *in vivo* antitumor effects of the dual insulin-like growth factor-I/insulin receptor inhibitor, BMS-554417. Cancer Res 2006;66:362–71.
16. Jones HE, Goddard L, Gee JM, et al. Insulin-like growth factor-I receptor signalling and acquired resistance to gefitinib (ZD1839; Iressa) in human breast and prostate cancer cells. Endocr Relat Cancer 2004;11:793–814.
17. Knowlden JM, Hutcheson IR, Barrow D, Gee JM, Nicholson RI. Insulin-like growth factor-I receptor signaling in tamoxifen-resistant breast cancer: a supporting role to the epidermal growth factor receptor. Endocrinology 2005;146:4609–18.
18. Lu Y, Zi X, Zhao Y, Mascarenhas D, Pollak M. Insulin-like growth factor-I receptor signaling and resistance to trastuzumab (Herceptin). J Natl Cancer Inst 2001;93: 1852–7.
19. Guix M, Faber AC, Wang SE, et al. Acquired resistance to EGFR tyrosine kinase inhibitors in cancer cells is mediated by loss of IGF-binding proteins. J Clin Invest 2008;118:2609–19.
20. Harris LN, You F, Schnitt SJ, et al. Predictors of resistance to preoperative trastuzumab and vinorelbine for HER2-positive early breast cancer. Clin Cancer Res 2007;13:1198–207.
21. Knowlden JM, Jones HE, Barrow D, Gee JM, Nicholson RI, Hutcheson IR. Insulin receptor substrate-1 involvement in epidermal growth factor receptor and insulin-like growth factor receptor signalling: implication for Gefitinib ('Iressa') response and resistance. Breast Cancer Res Treat 2008;111:79–91.
22. Perou CM, Sorlie T, Eisen MB, et al. Molecular portraits of human breast tumours. Nature 2000;406:747–52.

23. Sorlie T, Tibshirani R, Parker J, et al. Repeated observation of breast tumor subtypes in independent gene expression data sets. Proc Natl Acad Sci U S A 2003;100:8418–23.

24. van 't Veer LJ, Dai H, van de Vijver MJ, et al. Gene expression profiling predicts clinical outcome of breast cancer. Nature 2002;415:530–6.

25. Nielsen TO, Andrews HN, Cheang M, et al. Expression of the insulin-like growth factor I receptor and urokinase plasminogen activator in breast cancer is associated with poor survival: potential for intervention with 17-allylamino geldanamycin. Cancer Res 2004;64: 286–91.

26. Gee JM, Robertson JF, Gutteridge E, et al. Epidermal growth factor receptor/HER2/insulin-like growth factor receptor signalling and oestrogen receptor activity in clinical breast cancer. Endocr Relat Cancer 2005;12 Suppl 1:S99–111.

27. Pollak MN, Schernhammer ES, Hankinson SE. Insulin-like growth factors and neoplasia. Nat Rev Cancer 2004;4:505–18.

28. Garber K. IGF-1: old growth factor shines as new drug target. J Natl Cancer Inst 2005;97:790–2.

29. Makretsov N, Huntsman D, Nielsen T, et al. Hierarchical clustering analysis of tissue microarray immunostaining data identifies prognostically significant groups of breast carcinoma. Clin Cancer Res 2004; 10:6143–51.

30. Sutherland BW, Kucab J, Wu J, et al. Akt phosphorylates the Y-box binding protein 1 at Ser102 located in the cold shock domain and affects the anchorage-independent growth of breast cancer cells. Oncogene 2005;24:4281–92.

31. Kucab JE, Lee C, Chen CS, et al. Celecoxib analogues disrupt Akt signaling, which is commonly activated in primary breast tumours. Breast Cancer Res 2005;7:R796–807.

32. Sell C, Dumenil G, Deveaud C, et al. Effect of a null mutation of the insulin-like growth factor I receptor gene on growth and transformation of mouse embryo fibroblasts. Mol Cell Biol 1994;14:3604–12.

33. Stratford AL, Habibi G, Astanehe A, et al. Epidermal growth factor receptor (EGFR) is transcriptionally induced by the Y-box binding protein-1 (YB-1) and can be inhibited with Iressa in basal-like breast cancer, providing a potential target for therapy. Breast Cancer Res 2007;9:R61.

34. Berquin IM, Pang B, Dzuibinski ML, et al. Y-box binding protein 1 confers EGF independence to human mammary epithelial cells. Oncogene 2005;21:1–10.

35. To K, Zhao Y, Jiang H, et al. The phosphoinositide-dependent kinase-1 inhibitor, 2-amino-n-[4–5-(2-phenanthrenyl)-3-(trifluoromethyl)-1h-pyrazol-1-yl]-acetaminde (OSU03012) prevents Y-box binding protein-1 from inducing epidermal growth factor receptor. Mol Pharmacol 2007;72 no 3:641–52.

36. Wu J, Lee C, Yokom D, et al. Disruption of the Y-box binding protein-1 results in suppression of the epidermal growth factor receptor and HER-2. Cancer Res 2006; 66:4872–9.

37. Provenzano PP, Eliceiri KW, Campbell JM, Inman DR, White JG, Keely PJ. Collagen reorganization at the tumor-stromal interface facilitates local invasion. BMC Med 2006;4:38.

38. Iwenofu OH, Lackman RD, Staddon AP, Goodwin DG, Haupt HM, Brooks JS. Phospho-S6 ribosomal protein: a potential new predictive sarcoma marker for targeted mTOR therapy. Mod Pathol 2008;21:231–7.

39. Carriere A, Ray H, Blenis J, Roux PP. The RSK factors of activating the Ras/MAPK signaling cascade. Front Biosci 2008;13:4258–75.

40. Frodin M, Gammeltoft S. Role and regulation of 90 kDa ribosomal S6 kinase (RSK) in signal transduction. Mol Cell Endocrinol 1999;151:65–77.

41. Haluska P, Carboni JM, Teneyck C, et al. HER receptor signaling confers resistance to the insulin-like growth factor-I receptor inhibitor, BMS-536924. Mol Cancer Ther 2008;7:2589–98.

42. Smith JA, Poteet-Smith CE, Xu Y, Errington TM, Hecht SM, Lannigan DA. Identification of the first specific inhibitor of p90 ribosomal S6 kinase (RSK) reveals an unexpected role for RSK in cancer cell proliferation. Cancer Res 2005;65:1027–34.

43. Papa V, Costantino A, Belfiore A. Insulin receptor what role in breast cancer? Trends Endocrinol Metab 1997;8:306–12.

44. Chakraborty AK, Liang K, DiGiovanna MP. Co-targeting insulin-like growth factor I receptor and HER2: dramatic effects of HER2 inhibitors on nonoverexpressing breast cancer. Cancer Res 2008;68:1538–45.